

1 **Chronic corticosterone enhancement aggravates alpha-synuclein brain spreading pathology**  
2 **and substantia nigra neurodegeneration in mice**

3

4 Johannes Burtscher<sup>1</sup>, Jean-Christophe Copin<sup>1</sup>, João Rodrigues<sup>2</sup>, Senthil K. Thangaraj<sup>1</sup>, Anass  
5 Chiki<sup>1</sup>, Marie-Isabelle Guillot de Suduiraut<sup>2</sup>, Carmen Sandi<sup>2</sup>, & Hilal A. Lashuel<sup>\*1</sup>

6

7

8

9 1 Laboratory of Molecular and Chemical Biology of Neurodegeneration, Brain Mind Institute,  
10 EPFL, Switzerland

11 2 Laboratory of behavioral genetics, Brain Mind Institute, EPFL, Switzerland

12

13

14

15

16 \* To whom correspondences should be addressed: [hilal.lashuel@epfl.ch](mailto:hilal.lashuel@epfl.ch)

17 Key words: synuclein, Parkinson's disease, neurodegeneration, chronic stress, amygdala,  
18 phosphorylation, behavioral, pathology spreading

## 19 Abstract

20 Chronic stress and associated heightened glucocorticoid levels are risk factors for depression, a  
21 common non-motor symptom in Parkinson's disease (PD). However, how heightened  
22 glucocorticoids influence PD neuropathology [alpha-synuclein ( $\alpha$ -Syn) containing Lewy  
23 pathology and neurodegeneration] and disease progression is unclear. To address this  
24 knowledge gap, we investigated the impact of chronic corticosterone administration on  $\alpha$ -Syn  
25 pathology, neurodegeneration, behavior and mitochondrial function in a mouse model of  $\alpha$ -Syn  
26 pathology spreading after intracerebral injection of  $\alpha$ -Syn preformed fibrils (PFFs). Our results  
27 demonstrate that heightened corticosterone aggravates neurodegeneration and  $\alpha$ -Syn  
28 pathology spreading, intriguingly to specific brain regions, such as the entorhinal cortex.  
29 Corticosterone-treatment abolished distinct physiological adaptations after PFF-injection and  
30 induced differential physiological and behavioral consequences. Taken together, our work  
31 points to elevated glucocorticoids as a risk factor for the development of the neuropathological  
32 hallmarks of PD. Strategies aimed at reducing glucocorticoid levels might slow down pathology  
33 spreading and disease progression in synucleinopathy.

## 34 Introduction

35 Synucleinopathies, such as Parkinson's disease (PD), are diseases characterized by the  
36 accumulation and aggregation of the protein alpha-synuclein ( $\alpha$ -Syn) and neuronal loss in the  
37 affected brain regions (neocortical, limbic and nigro-striatal circuitries) <sup>1,2</sup>. Under physiological  
38 conditions,  $\alpha$ -Syn is believed to play roles in synaptic transmission <sup>3,4</sup>, exocytosis <sup>5</sup> and  
39 mitochondrial function <sup>6</sup>. In PD brains,  $\alpha$ -Syn undergoes conformational changes that render  
40 the protein prone to aggregation. Disease-associated mutations enhance  $\alpha$ -Syn aggregation *in-*  
41 *vitro* and promote the formation of Lewy body (LB) and Lewy neuritis-like pathology in neuronal  
42 and animal models of PD <sup>7</sup>. Studies using genetic manipulations of  $\alpha$ -Syn (either knockout or  
43 overexpressing different forms of  $\alpha$ -Syn) suggest that  $\alpha$ -Syn misfolding and aggregation, rather  
44 than loss of  $\alpha$ -Syn function, play central roles in the pathogenesis of PD and related  
45 synucleinopathies. This notion is supported by findings that mutations <sup>8-10</sup>, duplication <sup>11</sup> or  
46 triplication <sup>12</sup> of the gene coding for  $\alpha$ -Syn, *SNCA*, are sufficient to cause  $\alpha$ -Syn misfolding and  
47 aggregation and early onset forms of PD. Even though overexpression of WT or disease-  
48 associated mutants of  $\alpha$ -Syn in rodents or nonhuman primates recapitulate many pathological  
49 and motor features of PD, none of these models reproduce the full spectrum of pathological  
50 and clinical features of the disease <sup>13</sup>.

51 Besides the cardinal motor symptoms, non-motor symptoms are common in PD. Anxiety and  
52 depression disorders for example not only often precede PD, but represent common  
53 comorbidities and non-motor symptoms of PD at later stages <sup>14-16</sup>. PD-associated depression  
54 and anxiety have been linked to anatomical and metabolic alterations in the limbic system, in  
55 particular the amygdala, and the dopaminergic system <sup>17</sup>. The involvement of the amygdala in

56 stress effects, mood, emotion and reward behaviors is well-established<sup>18,19</sup>, and of interest also  
57 in the context of PD. Thus, the amygdala is particularly prone to the formation of  $\alpha$ -Syn  
58 pathology (LBs in PD-patients and LB-like pathology in many animal models)<sup>20,21</sup>, which occurs  
59 there as early as  $\alpha$ -Syn pathology is observed in the substantia nigra.

60 Recent findings showed the spreading of  $\alpha$ -Syn-pathology from host-tissues to mesencephalic  
61 transplants grafted into PD-patient's brains<sup>22,23</sup> and subsequent studies provided robust  
62 evidence for inter-neuronal transmission of  $\alpha$ -Syn-pathology<sup>24,25</sup>. Motivated by these  
63 observations, several groups sought to evaluate the hypothesis that  $\alpha$ -Syn-pathology can be  
64 induced by external seeds and be propagated through the central nervous system via a prion-  
65 like mechanism<sup>26-28</sup>. This hypothesis has been tested in rodents treated with different forms of  
66 recombinant  $\alpha$ -Syn aggregates (reviewed in<sup>29</sup>) or with  $\alpha$ -Syn aggregates derived from  
67 postmortem human brains from patients with  $\alpha$ -Syn-pathology, PD<sup>30</sup> or MSA<sup>31,32</sup>. Injection of  
68  $\alpha$ -Syn PFFs in different brain regions, such as the striatum<sup>27</sup>, the olfactory bulb<sup>33</sup> or the  
69 substantia nigra<sup>28</sup> induce pronounced  $\alpha$ -Syn pathology spreading, often strongest to the  
70 amygdala. Despite the observations of preferential accumulation of  $\alpha$ -Syn-pathology in the  
71 amygdala, literature linking  $\alpha$ -Syn-pathology spreading and amygdala-related behavior or  
72 physiology is sparse.

73  
74 Chronic stress and associated heightened glucocorticoid levels are known risk factors for  
75 anxiety and depression<sup>34,35</sup>, and have also been suggested to be risk factors for  
76 neurodegeneration in mouse PD models<sup>36,37</sup>. Therefore, we sought to investigate whether  
77 chronic elevation of corticosterone (CORT) would aggravate  $\alpha$ -Syn pathology spreading and

78 neurodegeneration after intrastriatal injection of  $\alpha$ -Syn PFFs. CORT was delivered in the  
79 drinking water over a period of 11 weeks to mice, a regime known to increase depression-like  
80 behaviours<sup>38-40</sup>. We then explored the possibility that chronic heightening of CORT and  $\alpha$ -Syn  
81 pathology synergistically increase behavioral deficits related to motor and non-motor  
82 symptoms of PD. Systemic administration of CORT has been demonstrated to increase the  
83 activity of the basolateral amygdala<sup>18</sup> and depression in PD is associated with increased  
84 metabolic activity in the amygdala<sup>17</sup>. Therefore, we also studied the metabolic and behavioral  
85 consequences of  $\alpha$ -Syn pathology in the amygdala.

86

## 87 Results

### 88 Experimental design and rationale

89 We generated PFFs from recombinant wild-type  $\alpha$ -Syn for intrastriatal injections in mice (suppl.  
90 Fig. 1). Analyses by transmission electron microscopy (TEM) revealed the presence of fibrils of  
91 different morphologies (suppl. Fig. 1a), including straight and twisted PFFs, resembling the  
92 heterogeneity of  $\alpha$ -Syn fibrils observed in human LB pathology<sup>41</sup>. As expected, the PFFs bound  
93 the amyloid-specific dye Thioflavin T and after sonication existed predominantly as short fibrils  
94 with a median length of 80 nm (suppl. Fig. 1b and 1c). The PFF preparations contained mainly  
95 fibrils, and 10-20% monomeric  $\alpha$ -Syn (suppl. Fig. 1d) that is generated during sonication and is  
96 in equilibrium with the fibrils through constant recycling of the monomers at the fibril ends<sup>42</sup>.  
97 This level of monomers was maintained in our preparations to enhance amyloid formation and  
98 the seeding capacity of the PFFs post injection<sup>43</sup>.

99 Our behavioral analyses focus on a time interval of 1-2 months after intrastriatal  $\alpha$ -Syn PFF  
100 injection. In our experiments, we consistently observe a peak of  $\alpha$ -Syn pS129-positive aggregate  
101 levels in the amygdala and cortical regions between 1 to 3 months after intrastriatal  $\alpha$ -Syn PFF  
102 injection (Fig. 1a). The main brain regions of interest were the striatum (site of PFF injection),  
103 the substantia nigra (neurodegeneration in which is crucial for cardinal motor symptoms in PD)  
104 and the amygdala (high pathology spreading). In the striatum,  $\alpha$ -Syn pS129 related pathology is  
105 predominantly neuritic 1 month after injection, whereas more peri-nuclear, compact, often  
106 half-moon shaped inclusions are observed at later time points (Fig. 1b, c), without observable  
107 loss of pS129 signal. To investigate the relationship between  $\alpha$ -Syn pathology and potential  
108 brain region related behavioral deficits in the time of highest  $\alpha$ -Syn aggregation load in the  
109 amygdala and other brain regions, behavioral tests were conducted 1-2 months after PFF  
110 injection.

111 Young adult, male mice were treated with CORT or vehicle, after which they were injected  
112 unilaterally with either  $\alpha$ -Syn PFFs [hereafter referred to as PFF(C) mice] or PBS [PBS(C) mice]  
113 into the dorsal striatum by stereotactic surgery. Vehicle treated mice are referred to as PBS-  
114 mice or PFF-mice, respectively. After surgery, CORT/vehicle treatment was continued until  
115 sacrifice (Fig. 2a). Half of the animals were used to assess mitochondrial parameters one month  
116 after PFF injection, the other half were subjected to behavioral testing followed by brain  
117 processing for histological analyses.

118 Treatment with CORT (Fig. 2a, suppl. Fig. 2a) induced depressive like phenotypes in the forced  
119 swim test (FST, suppl. Fig. 2b,c and 3) and in a saccharine preference test (suppl. Fig. 2d),  
120 indicating anhedonia-like behavior. Chronic CORT furthermore had pronounced effects on

121 weight gain after surgery and body fat content normalized to body weight (suppl. Fig. 2e,f,g), a  
122 well-known effect of elevated CORT-levels<sup>39,44</sup>, as well as on drinking and feeding behavior  
123 (suppl. Fig. 2h,i; note that CORT treatment was discontinued during activity measurements in  
124 the home cage, in which feeding and drinking behavior were dramatically changed). 2-way  
125 ANOVAs revealed significant effects of CORT treatment in the absence of PFF influences and  
126 interaction effects in all these parameters.

127

## 128 CORT-treatment aggravates $\alpha$ -Syn pathology spreading and dopaminergic cell 129 loss in $\alpha$ -Syn PFF-injected mice

130 We then investigated, whether the pathological hallmarks of PD –  $\alpha$ -Syn/Lewy-pathology and  
131 dopaminergic cell loss – are influenced by heightened corticosterone upon injection of PFFs.  
132  $\alpha$ -Syn pathology spreading was assessed histologically by densitometry of  $\alpha$ -Syn pS129  
133 immunoreactivity 60 days after PFF / PBS injection (Fig. 2b). No  $\alpha$ -Syn pS129 immunoreactivity  
134 was detected in PBS-injected controls. In PFF-injected animals, the highest  $\alpha$ -Syn pS129  
135 densities were observed in the hemisphere of injection in the amygdala, prelimbic cortex and  
136 substantia nigra for both, CORT and vehicle treated groups (Fig. 2b).  $\alpha$ -Syn pS129 signal in the  
137 entorhinal cortex was almost absent in the PFF group and significantly higher in the PFF(C)  
138 group. In the auditory cortex,  $\alpha$ -Syn pS129 density was significantly higher in PFF(C) mice (Fig.  
139 2c). No significant differences in spreading were observed in other brain regions (suppl. Fig. 4).  
140 60 days after PFF-injection, no dopaminergic cell loss in the substantia nigra was observed in  
141 PFF mice. On the other hand, CORT treatment resulted in decreased density of tyrosine-  
142 hydroxylase (TH) immunoreactivity and reduced ipsilateral (hemisphere of injection) to

143 contralateral TH-positive cell numbers in the hemisphere of PFF-injection as compared to the  
144 contralateral substantia nigra (Fig. 3a-d); no such effects were observed in PBS-injected groups  
145 (suppl. Fig. 5a-c). The density for  $\alpha$ -Syn pS129-positive aggregates (Fig. 3e,f) and colocalization  
146 of pS129 with TH (suppl. Fig. 5d) were similar between PFF and PFF(C) animals.  $\alpha$ -Syn pS129-  
147 positive aggregates colocalized with the macro autophagy marker p62 and ubiquitin in in the  
148 substantia nigra of PFF and PFF(C) mice (suppl. Fig. 6), and in other brain regions (suppl. Fig. 7).  
149 The aggregates were resistant to proteinase K treatment and were detected by antibodies for  
150 pS129 and for the N-terminal part of  $\alpha$ -Syn (1-20) (Fig. 3g). Motor coordination in the rotarod  
151 test was significantly reduced in PFF(C) mice, but was mainly due to CORT treatment, and not  
152 due to PFF or interaction (suppl. Fig. 5f). Total distance travelled during 3 days in the activity  
153 cage (AC) was similar across groups (suppl. Fig. 5e). Altogether, these results suggest that  
154 chronic CORT-treatment aggravated substantia nigra neurodegeneration after PFF injection  
155 without affecting pS129 immunoreactivity quantitatively (Fig. 3f) or qualitatively (Fig. 3g and  
156 suppl. Fig. 6), general motor behavior in the AC or motor coordination in this time interval.

157

## 158 CORT-treatment reverses anxiety-effects of $\alpha$ -Syn PFF injection

159 Elevated CORT has been shown to affect mood and emotional behavior<sup>38-40</sup>, and Chronic CORT  
160 also affects depressive-like behavior, independently of PFF injection (Fig. 2). Given our  
161 observation of pronounced  $\alpha$ -Syn pathology in several brain regions implicated in mood and  
162 emotional behavior, such as the amygdala (Fig. 1, 2), we also investigated anxiety-like  
163 behaviors. We assessed basal spontaneous anxiety and exploratory reactivity to novelty in the  
164 elevated plus maze (EPM) and open field test (OF). The OF was followed by a novel object test,



165 assessing anxiety-linked novelty seeking. No differences in all these anxiety parameters were  
166 observed between PBS-injected groups (suppl. Fig. 8a-i). However, we observed a moderate  
167 hypo-anxious phenotype for PFF mice in the EPM, which was reversed by CORT-treatment (Fig.  
168 4a-f). PFF(C) animals also moved less in the EPM (Fig. 4d). In the OF, a similar effect was  
169 observed (Fig. 4g,h): PFF-injection induced hypo-anxious phenotypes (more time spent in the  
170 center and less time spent at the walls of the arena), which was reversed by chronic CORT-  
171 treatment, resulting in statistically different behavior in the OF between the PFF-injected  
172 groups. The mice in all groups moved at similar speed in this test (Fig. 4i). Neither CORT-  
173 treatment, nor PFF-injection significantly impacted on the interest in a novel object (suppl. Fig.  
174 8j-m). A marble burying test, used to assess neophobia and anxiety, revealed no differences  
175 across groups (suppl. Fig. 9a,b). Taken together, PFF-injection resulted in a moderately hypo-  
176 anxious phenotype, which was reversed by CORT-treatment, in the EPM even trending towards  
177 hyper-anxious phenotypes.

178

## 179 $\alpha$ -Syn pathology in the amygdala does not alter mitochondrial respirational 180 capacities, fear behavior or aggression

181 We observed the highest levels of  $\alpha$ -Syn pathology of all brain regions in the ipsilateral  
182 amygdala (hemisphere of injection) of PFF(C) animals (Fig. 2b).  $\alpha$ -Syn pS129 levels, assessed by  
183 immunostaining (Fig. 5a,b) were not significantly different in the amygdala of PFF and PFF(C)  
184 mice. We hypothesized that the aggregation load in the amygdala should negatively impact on  
185 its physiology. Due to the involvement of the amygdala in fear-related and aggressive behavior  
186 <sup>45,46</sup>, we assessed potential impairment of these behaviors applying a fear conditioning protocol

187 and a resident intruder aggression test. As monomeric and aggregated  $\alpha$ -Syn species have been  
188 shown to affect mitochondrial function, we hypothesized that  $\alpha$ -Syn pathology might disturb  
189 mitochondrial functions in the amygdala. More specifically, the mitochondrial import  
190 machinery<sup>47</sup>, mitochondrial membrane potential, cytochrome c release, ROS and morphology  
191<sup>48,49</sup> as well as mitochondrial permeability transition pore and electron transfer system  
192 regulation<sup>6,50</sup> have all been implicated to be affected by  $\alpha$ -Syn. We observed, however, no  
193 adverse effect of amygdala  $\alpha$ -Syn pathology on mitochondrial functions *in vivo*. Mitochondrial  
194 respiration (Fig. 5c, suppl. Fig. 10), mitochondrial ROS-production (Fig. 5d, suppl. Fig. 10), flux  
195 control ratios (suppl. Fig. 11e) and oxidative phosphorylation coupling efficiency (respiratory  
196 control ratio, RCR) (suppl. Fig. 12b) did not differ across groups (controls and contralateral data  
197 in suppl. Fig. 10). Notably, at the site of PFF-injection (striatum), we observed a significantly  
198 higher reliance of mitochondrial respiration on the succinate pathway of PFF mice as compared  
199 to PFF(C) mice (suppl. Fig. 13e,f). PFF and PFF(C) mice also did not behave differently compared  
200 to PBS-injected controls in fear conditioning (Fig. 5f,g and suppl. Fig. 14) and resident intruder  
201 tests (suppl. Fig. 15). Thus,  $\alpha$ -Syn pathology does not appear to significantly impair amygdala  
202 mitochondrial physiology or amygdala-related behaviors.

203

## 204 Discriminant analysis reveals differential effects of $\alpha$ -Syn PFFs in heightened 205 CORT conditions

206 To investigate in more detail the relations of  $\alpha$ -Syn, CORT-treatment and behavioral  
207 components, partial least squares (PLS) discriminant analysis was performed (Fig. 6). The 6  
208 variables with highest variable importance in projection (VIP) for each component used in a 2-

209 component model (Fig. 6a) were identified (body fat content, weight gain, behavior in the FST,  
210 as well as drinking, feeding and hedonic behavior in the AC), yielding good predictive capacity  
211 for the CORT condition (Fig. 6b). The heatmap in 6c depicts the relatively faithful prediction of  
212 VIP variables, and scatterplots in 6d reveal good separation of the PFF(C) mice from other  
213 treatment groups.

214

### 215 Correlation of $\alpha$ -Syn pathology with behavioral phenotypes

216 Next, we sought to investigate, whether brain-region specific  $\alpha$ -Syn pathology correlated with  
217 the performance in behavioral tests. We observed several significant correlations (Fig. 7). Due  
218 to the absence of  $\alpha$ -Syn pS129 immunoreactivity in PBS-injected controls, only PFF-injected  
219 animals were subjected to correlation analyses. CORT and vehicle pretreated cohorts exhibited  
220 differential correlation patterns. For example, substantia nigra  $\alpha$ -Syn pS129 density correlated  
221 to several behavioral parameters in the CORT, but not the vehicle group (suppl. Fig. 16).

222

223 We applied partial least squares (PLS) regression analysis, followed by multivariate ANOVA to  
224 further elucidate the dependent behavioral variables predicting  $\alpha$ -Syn pathology in different  
225 brain regions (Fig. 8). Mean values of  $\alpha$ -Syn pS129 immunoreactivity (% of area) for selected  
226 brain regions (PFF and PFF(C) mice pooled) were used to select additional brain regions with  
227 high  $\alpha$ -Syn pathology (8a), beside regions of main *a-priori* interest (striatum, substantia nigra,  
228 amygdala) and the entorhinal cortex that emerged of being most affected by CORT-treatment  
229 after PFF-injection. Components for all PFF-injected mice (PFF and PFF(C) mice pooled) were  
230 calculated and used to extract differences between PFF and PFF(C) mice (8b). The resulting

231 models explained 15-25 % of variability for several selected brain regions (Fig. 8c, upper panel).  
232 Scores of behavioral and physiological outcomes on the components are depicted in Fig. 8c  
233 (lower panel). Interpretation example: striatum component 1 (Fig. 8c) explains that  $\alpha$ -Syn  
234 pathology of the striatum was associated with lower values of consumed food in the AC,  
235 saccharine preference in the AC, velocity in the EPM, and in the OF. While PFF(C) mice had  
236 positive scores on striatum component 1, PFF mice scored negatively (Fig. 8b). Therefore, the  
237 CORT intervention impacted negatively on these striatum-related behaviors.

238

## 239 Discussion

240 Despite profound impact on quality of patient life <sup>51</sup>, non-motor symptoms, including affective  
241 disorders, remain less well characterized compared to motor symptoms and their impact on PD  
242 pathology and disease progression remains unknown. Several previous studies in rodent  
243 models of PD fortified the link with affective disorders <sup>52 53</sup>. Chronic mild stress induced  
244 depression was also shown to worsen neurochemical and behavioral outcomes in the MPTP (1-  
245 Methyl-4-phenyl-1,2,3,6-tetrahydropyridin) model of PD <sup>54</sup>. Chronic stress and stress-associated  
246 heightened glucocorticoid levels are known risk factors for these affective disorders <sup>34,35</sup>, and  
247 potential risk factors for neurodegeneration, as has been demonstrated in mouse PD models  
248 <sup>36,37</sup>. Despite the associations between glucocorticoid levels, affective disorders and PD, the  
249 relationship of models of (depression-inducing) heightened glucocorticoid and  $\alpha$ -Syn pathology  
250 spreading has not been assessed previously. On the bases of these observations, we  
251 hypothesized that heightened CORT levels could influence  $\alpha$ -Syn pathology and

252 neurodegeneration in PD and sought to test this hypothesis in the well-established mouse  
253 model of  $\alpha$ -Syn pathology spreading induced by intrastriatal injection of  $\alpha$ -Syn PFFs.  
254 We report aggravated  $\alpha$ -Syn pathology spreading and neurodegeneration at chronic CORT  
255 administration and after PFF injection. These effects coincided with differential behavioural  
256 effects as compared to PFF-injected mice without CORT treatment.

257

### 258 CORT-treatment aggravates $\alpha$ -Syn pathology spreading and dopaminergic cell 259 loss in $\alpha$ -Syn PFF-injected mice

260 Unilateral injection of  $\alpha$ -Syn PFFs into the striatum caused pronounced pathology spreading to  
261 various brain regions two months later.  $\alpha$ -Syn pathology spreading was aggravated in distinct  
262 brain regions after CORT pretreatment, most notably in the entorhinal cortex. Interestingly, the  
263 entorhinal cortex is severely affected by Lewy pathology in many PD<sup>55,56</sup> and dementia with LB  
264<sup>57</sup> patients. We observed that the entorhinal cortex  $\alpha$ -Syn pathology was significantly correlated  
265 with several behavioral measures assessed, including depressive-like behavior in the FST, motor  
266 behavior in the EPM and saccharine preference. Our results point to the entorhinal cortex as  
267 being a particularly vulnerable brain region for  $\alpha$ -Syn pathology in conditions of glucocorticoid  
268 dysbalance.  $\alpha$ -Syn pathology in this region after PFF-injection of vehicle-pretreated animals was  
269 sparse or absent, but considerable pS129 pathology was observed in all PFF(C) mice. Due to the  
270 entorhinal cortex' prominent role in cognition and potential role of entorhinal Lewy pathology  
271 in cognitive deficits in PD<sup>55,58</sup>, studies on PD patients assessing the effect of chronic stress and  
272 depression on cognitive performance and  $\alpha$ -Syn pathology in the entorhinal cortex will be of  
273 interest.

274 No neuronal loss in the substantia nigra was observed in PFF mice, which is in line with previous  
275 reports, in which neurodegeneration is detected only ~ 180 days after injection<sup>27</sup>. PFF(C) mice  
276 presented with reduced tyrosine hydroxylase (TH) immunoreactivity and a decreased ratio of  
277 TH-positive neurons in the substantia nigra (pars compacta & reticulata) of the hemisphere of  
278 injection as compared to the contralateral hemisphere.  $\alpha$ -Syn pS129 pathology in the  
279 substantia nigra was not different between CORT or vehicle treated mice. These findings  
280 demonstrate that heightened CORT-levels aggravated  $\alpha$ -Syn pathology spreading and nigral  
281 neurodegeneration following intrastriatal PFF injection.

282

### 283 **CORT-treatment reverses anxiety-effects of $\alpha$ -Syn PFF injection**

284 Chronic CORT treatment induced depressive-like phenotypes and pronounced physiological  
285 changes, independent of PFF injection. CORT treatment surprisingly reversed hypo-anxious-like  
286 behavior induced by  $\alpha$ -Syn PFF injection in the EPM and OF. This finding seems particularly  
287 relevant as hypo-anxiety is a common observation in models of early stages of PD<sup>59,60</sup>, and  
288 might reflect changes in dopamine signalling<sup>61</sup>. We speculate that chronic CORT treatment  
289 impaired dynamic adaptations to  $\alpha$ -Syn pathology, thereby preventing potential transient  
290 bursts in dopamine signaling, that might occur due to  $\alpha$ -Syn's suspected function as negative  
291 regulator of dopamine release<sup>4,62</sup>. In line with this assumption is a recent report on enhanced  
292 presynaptic activity of neurons in presence of  $\alpha$ -Syn inclusions<sup>63</sup>. Such dynamic adaptations  
293 might comprise shifts in the contributions of mitochondrial respiration pathways, as observed  
294 in the striatum. PFF animals exhibited increased relative contribution of the succinate pathway  
295 to overall mitochondrial respiration as compared to PFF(C) mice. Impairment of succinate

296 dehydrogenase activity in the striatum has been linked to excitotoxicity<sup>64</sup> and protocols of  
297 succinate dehydrogenase inhibition (“chemical preconditioning”) have been shown to induce  
298 neuroprotection<sup>65</sup>, suggesting its involvement in neuroprotective adaptations following  
299 challenges. Therefore, our findings support the view that  $\alpha$ -Syn pathology at early time points  
300 (1-2 months) after injection of PFFs is associated with adaptive changes in the striatum. Such  
301 adaptations could include a shift of mitochondrial respiration towards (potentially protective)  
302 stronger reliance on succinate- / mitochondrial Complex II-linked respiration ( $S_E$ ), which is  
303 blocked by chronic CORT. Interestingly, the effect size of  $S_E$  FCR between PFF(C) and PFF groups  
304 is comparable to the differences observed in anxiety-like behaviors, behaviors with important  
305 striatal participation<sup>66</sup>.

306 In summary, we report that alterations in anxiety- and depression-like behaviour due to  $\alpha$ -Syn  
307 pathology were not exacerbated by our heightened CORT treatment. Whereas depressive-like  
308 phenotypes were solely attributable, in a non-additive manner, to CORT treatment, CORT  
309 reversed PFF-induced changes in anxiety-like behaviour in some tests (EPM, OF).

310

### 311 $\alpha$ -Syn pathology in the amygdala does not alter mitochondrial respirational 312 capacities, fear behavior or aggression

313 A high level of  $\alpha$ -Syn pathology in the amygdala has been reported in patients suffering from PD  
314 and other neurodegenerative diseases<sup>21</sup>, as well as in several  $\alpha$ -Syn pathology spreading  
315 models<sup>27,28,30,33</sup>. The amygdala is importantly involved in emotional behavior and depression in  
316 general<sup>19</sup> and in PD in particular<sup>51</sup>. Therefore, we sought to determine, whether chronic CORT

317 treatment would aggravate associated symptoms in a widely used  $\alpha$ -Syn pathology spreading  
318 mouse model, in particular related to the amygdala.

319 We observed a similar strong pathology spreading to the amygdala following PFF injection,  
320 irrespective of CORT treatment. Despite the severe  $\alpha$ -Syn pathology observed in PFF-treated  
321 animals, several amygdala-related behaviors (e.g., fear-related behaviors, aggression) were  
322 unaffected. Furthermore, PFF treatment did not affect several mitochondrial parameters  
323 measured in the amygdala. Taken together, these results suggest that  $\alpha$ -Syn aggregations by  
324 themselves are not immediately toxic. This finding is in line with recent observations that  
325 hippocampus-dependent behavior is not altered by the induction of severe hippocampal  $\alpha$ -Syn  
326 pathology either<sup>67</sup>. Alternatively, it is possible that, at the time points following treatments at  
327 which the current study took place, the relevant neuronal circuits are resilient or plastic enough  
328 to prevent general physiological deterioration or behavioral alterations. Over time only some  
329 particularly vulnerable neuronal populations – such as TH-neurons in the substantia nigra –  
330 succumb to degeneration. As previously suggested<sup>68</sup> for primary neurons seeded with PFFs,  
331 toxicity might be conferred to the aggregations in presence of additional insult factors or after  
332 more advanced maturation (into LBs).

333

### 334 [Correlation studies of behavior and pS129 immunoreactivity](#)

335 The finding of small effects of  $\alpha$ -Syn pathology on amygdala physiology prompted us to further  
336 investigate potential correlations of  $\alpha$ -Syn pathology in other brain regions with behavior and  
337 physiological parameters. We determined several such parameters by discriminant analysis,  
338 differentiating the PFF(C) condition better than the PFF condition from controls. This supports



339 again the notion, that  $\alpha$ -Syn pathology by itself does not strongly impact on behavior. To  
340 investigate potential correlations of  $\alpha$ -Syn pathology in distinct brain regions with behavioral  
341 outcomes more closely, we created correlation matrices for behavioral and physiological  
342 outcomes with  $\alpha$ -Syn pathology in specific brain regions. pS129 immunoreactivity in the  
343 entorhinal cortex for PFF-injected –including PFF-injected CORT-treated– mice was negatively  
344 correlated with feeding, drinking, hedonic behavior and movement in the EPM, whereas  
345 positive correlations were observed for body fat content and depressive-like behavior in the  
346 FST, which is interesting in the light of anti-depressive effects demonstrated by activation of the  
347 entorhinal cortex<sup>69</sup>. Correlation patterns for FST and AC parameters were intriguingly inverted  
348 in the visual, as compared to the entorhinal cortex. Substantia nigra  $\alpha$ -Syn pathology was  
349 correlated with motor behaviors: negatively with distance travelled in the AC (similar effects of  
350 somatosensory and cingulate cortices, but – surprisingly – positively with performance on the  
351 Rotarod.  $\alpha$ -Syn pathology in the amygdala coincided with reduced explorative behavior in the  
352 EPM and with reduced drinking. These results were essentially confirmed by PLS regression  
353 analysis, which strikingly separated PFF and PFF(C) groups in all analyzed brain regions very  
354 clearly; in this model regarding  $\alpha$ -Syn pathology in the substantia nigra, we identified  
355 additionally increased associated fear behaviors (freezing in the cue and context test), (non-  
356 aggressive) sniffing behavior in the resident intruder test and anxiety like behavior in the OF  
357 (latency to enter the center) as more positively correlated with CORT treatment. Interestingly,  
358 pS129 immunoreactivity in the prelimbic cortex, which was among the highest among all brain  
359 regions; was differentially associated with aggressive and fear behaviors (more negatively  
360 associated in PFF(C) mice), as well as with body fat content and weight gain (more positively

361 associated in PFF(C) mice). Similar to the effect of the reversal of hypo-anxiety-like behavior in  
362 the EPM and OF by CORT treatment, these correlative results demonstrate divergent  
363 physiological and behavioral alterations in heightened CORT conditions in PFF-injected mice,  
364 potentially mediated by CORT-suppressed beneficial adaptations (shift to complex-I linked  
365 respiration, hypo-anxiety), leading to higher vulnerability of PFF(C) mice to  $\alpha$ -Syn pathology and  
366 neurodegeneration. These adaptations did not appear to be linked to differential  
367 neuroinflammation, as increased astrogliosis was only observed at the site of injection of PFF  
368 and was not modulated by CORT (suppl. Fig. 17).

369

## 370 Conclusions

371 We report aggravated  $\alpha$ -Syn pathology spreading and neurodegeneration in mice injected with  
372  $\alpha$ -Syn PFFs, in a condition of heightened CORT. This suggests heightened glucocorticoid levels  
373 risk factor for the development of the neuropathological hallmarks of PD and potential target  
374 for treatment. Taken together, our findings suggest that chronic CORT-treatment reduces the  
375 ability of the mouse brain to adapt to the additional proteostatic stress of intrastriatal injection  
376 of  $\alpha$ -Syn PFFs, resulting in lower thresholds for  $\alpha$ -Syn pathology handling and nigral  
377 neurodegeneration. Further elucidation of (molecular) vulnerability factors of specific brain  
378 regions to  $\alpha$ -Syn pathology, and why at some point resilience fails and neurodegeneration (such  
379 as in the substantia nigra) occurs, will be of importance to understand the complex effects of  $\alpha$ -  
380 Syn pathology. Based on our results, we suggest that  $\alpha$ -Syn pathology in absence of additional  
381 clinical (such as depression, chronic stress and potentially anxiety, sleep disturbances, etc) and  
382 molecular (reduced mitochondrial function, reduced anti-oxidative capacities, etc.) risk factors

383 is not immediately noxious, maybe even triggering transient protective adaptations. This is in  
384 line with reported inconsistencies of LB-pathology and clinical symptoms in human patients and  
385 moderate reflection of general PD-symptomatology in  $\alpha$ -Syn-based rodent models<sup>70</sup>.

386

387

388 Acknowledgments: We are grateful to Ioannis Zalachoras, Laia Morató Fornaguera, Anne  
389 Michel, Georges Mairet-Coello, Rachel Angers, Patrick Downey and Martin Citron for valuable  
390 intellectual inputs. We thank the following core facilities of the EPFL for excellent technical  
391 assistance: Phenotyping Unit (UDP), Histology Core Facility (HCF) and Bioimaging and Optics  
392 Platform (BIOP). This work was funded by UCB S.A. and EPFL.

393 Author contributions: *JB*: Conceptualization, Data curation, Formal analysis, Investigation,  
394 Writing – original draft, *JCC*: Conceptualization, Data curation, Formal analysis, Investigation, *JR*:  
395 Formal analysis, *SKT*, *AC*, *IGS*: Data curation, Formal analysis, *CS*: Conceptualization, Formal  
396 analysis, Writing – original draft, *HAL*: Conceptualization, Formal analysis, Funding acquisition,  
397 Writing – original draft

398 All authors reviewed, edited and approved of the manuscript.

399 Competing interests: the presented work was partly funded by UCB S.A.

## 400 References

- 401 1 Spillantini, M. G. *et al.* Alpha-synuclein in Lewy bodies. *Nature* **388**, 839-840, doi:10.1038/42166  
402 (1997).
- 403 2 Lashuel, H. A., Overk, C. R., Oueslati, A. & Masliah, E. The many faces of alpha-synuclein: from  
404 structure and toxicity to therapeutic target. *Nature reviews. Neuroscience* **14**, 38-48,  
405 doi:10.1038/nrn3406 (2013).
- 406 3 Burre, J. *et al.* Alpha-synuclein promotes SNARE-complex assembly in vivo and in vitro. *Science*  
407 (*New York, N.Y.*) **329**, 1663-1667, doi:10.1126/science.1195227 (2010).
- 408 4 Abeliovich, A. *et al.* Mice lacking alpha-synuclein display functional deficits in the nigrostriatal  
409 dopamine system. *Neuron* **25**, 239-252 (2000).
- 410 5 Logan, T., Bendor, J., Toupin, C., Thorn, K. & Edwards, R. H. alpha-Synuclein promotes dilation of  
411 the exocytotic fusion pore. *Nature neuroscience* **20**, 681-689, doi:10.1038/nn.4529 (2017).
- 412 6 Ludtmann, M. H. *et al.* Monomeric Alpha-Synuclein Exerts a Physiological Role on Brain ATP  
413 Synthase. *The Journal of neuroscience : the official journal of the Society for Neuroscience* **36**,  
414 10510-10521, doi:10.1523/jneurosci.1659-16.2016 (2016).
- 415 7 Polymenidou, M. & Cleveland, D. W. Prion-like spread of protein aggregates in  
416 neurodegeneration. *The Journal of experimental medicine* **209**, 889-893,  
417 doi:10.1084/jem.20120741 (2012).
- 418 8 Polymeropoulos, M. H. *et al.* Mutation in the alpha-synuclein gene identified in families with  
419 Parkinson's disease. *Science (New York, N.Y.)* **276**, 2045-2047 (1997).
- 420 9 Kruger, R. *et al.* Ala30Pro mutation in the gene encoding alpha-synuclein in Parkinson's disease.  
421 *Nature genetics* **18**, 106-108, doi:10.1038/ng0298-106 (1998).
- 422 10 Zarranz, J. J. *et al.* The new mutation, E46K, of alpha-synuclein causes Parkinson and Lewy body  
423 dementia. *Annals of neurology* **55**, 164-173, doi:10.1002/ana.10795 (2004).

- 424 11 Singleton, A. B. *et al.* alpha-Synuclein locus triplication causes Parkinson's disease. *Science (New*  
425 *York, N.Y.)* **302**, 841, doi:10.1126/science.1090278 (2003).
- 426 12 Ibanez, P. *et al.* Causal relation between alpha-synuclein gene duplication and familial  
427 Parkinson's disease. *Lancet (London, England)* **364**, 1169-1171, doi:10.1016/s0140-  
428 6736(04)17104-3 (2004).
- 429 13 Dawson, T. M., Golde, T. E. & Lagier-Tourenne, C. Animal models of neurodegenerative diseases.  
430 *Nature neuroscience* **21**, 1370-1379, doi:10.1038/s41593-018-0236-8 (2018).
- 431 14 Kalia, L. V. & Lang, A. E. Parkinson's disease. *Lancet (London, England)* **386**, 896-912,  
432 doi:10.1016/s0140-6736(14)61393-3 (2015).
- 433 15 Shiba, M. *et al.* Anxiety disorders and depressive disorders preceding Parkinson's disease: a  
434 case-control study. *Movement disorders : official journal of the Movement Disorder Society* **15**,  
435 669-677 (2000).
- 436 16 Sagna, A., Gallo, J. J. & Pontone, G. M. Systematic review of factors associated with depression  
437 and anxiety disorders among older adults with Parkinson's disease. *Parkinsonism & related*  
438 *disorders* **20**, 708-715, doi:10.1016/j.parkreldis.2014.03.020 (2014).
- 439 17 Thobois, S., Prange, S., Sgambato-Faure, V., Tremblay, L. & Broussolle, E. Imaging the Etiology of  
440 Apathy, Anxiety, and Depression in Parkinson's Disease: Implication for Treatment. *Current*  
441 *neurology and neuroscience reports* **17**, 76, doi:10.1007/s11910-017-0788-0 (2017).
- 442 18 Kavushansky, A. & Richter-Levin, G. Effects of stress and corticosterone on activity and plasticity  
443 in the amygdala. *Journal of neuroscience research* **84**, 1580-1587, doi:10.1002/jnr.21058 (2006).
- 444 19 Janak, P. H. & Tye, K. M. From circuits to behaviour in the amygdala. *Nature* **517**, 284-292,  
445 doi:10.1038/nature14188 (2015).

- 446 20 Popescu, A., Lippa, C. F., Lee, V. M. & Trojanowski, J. Q. Lewy bodies in the amygdala: increase of  
447 alpha-synuclein aggregates in neurodegenerative diseases with tau-based inclusions. *Archives of*  
448 *neurology* **61**, 1915-1919, doi:10.1001/archneur.61.12.1915 (2004).
- 449 21 Nelson, P. T. *et al.* The Amygdala as a Locus of Pathologic Misfolding in Neurodegenerative  
450 Diseases. *Journal of neuropathology and experimental neurology* **77**, 2-20,  
451 doi:10.1093/jnen/nlx099 (2018).
- 452 22 Kordower, J. H., Chu, Y., Hauser, R. A., Freeman, T. B. & Olanow, C. W. Lewy body-like pathology  
453 in long-term embryonic nigral transplants in Parkinson's disease. *Nature medicine* **14**, 504-506,  
454 doi:10.1038/nm1747 (2008).
- 455 23 Li, J. Y. *et al.* Lewy bodies in grafted neurons in subjects with Parkinson's disease suggest host-  
456 to-graft disease propagation. *Nature medicine* **14**, 501-503, doi:10.1038/nm1746 (2008).
- 457 24 Desplats, P. *et al.* Inclusion formation and neuronal cell death through neuron-to-neuron  
458 transmission of alpha-synuclein. *Proceedings of the National Academy of Sciences of the United*  
459 *States of America* **106**, 13010-13015, doi:10.1073/pnas.0903691106 (2009).
- 460 25 Volpicelli-Daley, L. A. *et al.* Exogenous alpha-synuclein fibrils induce Lewy body pathology  
461 leading to synaptic dysfunction and neuron death. *Neuron* **72**, 57-71,  
462 doi:10.1016/j.neuron.2011.08.033 (2011).
- 463 26 Mougenot, A. L. *et al.* Prion-like acceleration of a synucleinopathy in a transgenic mouse model.  
464 *Neurobiology of aging* **33**, 2225-2228, doi:10.1016/j.neurobiolaging.2011.06.022 (2012).
- 465 27 Luk, K. C. *et al.* Pathological alpha-synuclein transmission initiates Parkinson-like  
466 neurodegeneration in nontransgenic mice. *Science (New York, N.Y.)* **338**, 949-953,  
467 doi:10.1126/science.1227157 (2012).
- 468 28 Masuda-Suzukake, M. *et al.* Prion-like spreading of pathological alpha-synuclein in brain. *Brain :*  
469 *a journal of neurology* **136**, 1128-1138, doi:10.1093/brain/awt037 (2013).

- 470 29 Rey, N. L., George, S. & Brundin, P. Review: Spreading the word: precise animal models and  
471 validated methods are vital when evaluating prion-like behaviour of alpha-synuclein.  
472 *Neuropathology and applied neurobiology* **42**, 51-76, doi:10.1111/nan.12299 (2016).
- 473 30 Recasens, A. *et al.* Lewy body extracts from Parkinson disease brains trigger alpha-synuclein  
474 pathology and neurodegeneration in mice and monkeys. *Annals of neurology* **75**, 351-362,  
475 doi:10.1002/ana.24066 (2014).
- 476 31 Prusiner, S. B. *et al.* Evidence for alpha-synuclein prions causing multiple system atrophy in  
477 humans with parkinsonism. *Proceedings of the National Academy of Sciences of the United*  
478 *States of America* **112**, E5308-5317, doi:10.1073/pnas.1514475112 (2015).
- 479 32 Peng, C. *et al.* Cellular milieu imparts distinct pathological alpha-synuclein strains in alpha-  
480 synucleinopathies. *Nature*, doi:10.1038/s41586-018-0104-4 (2018).
- 481 33 Rey, N. L. *et al.* Widespread transneuronal propagation of alpha-synucleinopathy triggered in  
482 olfactory bulb mimics prodromal Parkinson's disease. *The Journal of experimental medicine* **213**,  
483 1759-1778, doi:10.1084/jem.20160368 (2016).
- 484 34 Sandi, C. & Richter-Levin, G. From high anxiety trait to depression: a neurocognitive hypothesis.  
485 *Trends in neurosciences* **32**, 312-320, doi:10.1016/j.tins.2009.02.004 (2009).
- 486 35 de Kloet, E. R. *et al.* Stress and Depression: a Crucial Role of the Mineralocorticoid Receptor.  
487 *Journal of neuroendocrinology* **28**, doi:10.1111/jne.12379 (2016).
- 488 36 Hemmerle, A. M., Dickerson, J. W., Herman, J. P. & Seroogy, K. B. Stress exacerbates  
489 experimental Parkinson's disease. *Molecular psychiatry* **19**, 638-640, doi:10.1038/mp.2013.108  
490 (2014).
- 491 37 Wu, Q., Yang, X., Zhang, Y., Zhang, L. & Feng, L. Chronic mild stress accelerates the progression  
492 of Parkinson's disease in A53T alpha-synuclein transgenic mice. *Experimental neurology* **285**, 61-  
493 71, doi:10.1016/j.expneurol.2016.09.004 (2016).

- 494 38 Gourley, S. L., Kiraly, D. D., Howell, J. L., Olausson, P. & Taylor, J. R. Acute hippocampal brain-  
495 derived neurotrophic factor restores motivational and forced swim performance after  
496 corticosterone. *Biological psychiatry* **64**, 884-890, doi:10.1016/j.biopsych.2008.06.016 (2008).
- 497 39 David, D. J. *et al.* Neurogenesis-dependent and -independent effects of fluoxetine in an animal  
498 model of anxiety/depression. *Neuron* **62**, 479-493, doi:10.1016/j.neuron.2009.04.017 (2009).
- 499 40 Bacq, A. *et al.* Organic cation transporter 2 controls brain norepinephrine and serotonin  
500 clearance and antidepressant response. *Molecular psychiatry* **17**, 926-939,  
501 doi:10.1038/mp.2011.87 (2012).
- 502 41 Spillantini, M. G., Crowther, R. A., Jakes, R., Hasegawa, M. & Goedert, M. alpha-Synuclein in  
503 filamentous inclusions of Lewy bodies from Parkinson's disease and dementia with lewy bodies.  
504 *Proceedings of the National Academy of Sciences of the United States of America* **95**, 6469-6473  
505 (1998).
- 506 42 Carulla, N. *et al.* Molecular recycling within amyloid fibrils. *Nature* **436**, 554-558,  
507 doi:10.1038/nature03986 (2005).
- 508 43 Mahul-Mellier, A. L. *et al.* Fibril growth and seeding capacity play key roles in alpha-synuclein-  
509 mediated apoptotic cell death. *Cell death and differentiation* **22**, 2107-2122,  
510 doi:10.1038/cdd.2015.79 (2015).
- 511 44 Rebuffe-Scrive, M., Walsh, U. A., McEwen, B. & Rodin, J. Effect of chronic stress and exogenous  
512 glucocorticoids on regional fat distribution and metabolism. *Physiology & behavior* **52**, 583-590  
513 (1992).
- 514 45 Rogan, M. T., Staubli, U. V. & LeDoux, J. E. Fear conditioning induces associative long-term  
515 potentiation in the amygdala. *Nature* **390**, 604-607, doi:10.1038/37601 (1997).



- 516 46 Coccaro, E. F., McCloskey, M. S., Fitzgerald, D. A. & Phan, K. L. Amygdala and orbitofrontal  
517 reactivity to social threat in individuals with impulsive aggression. *Biological psychiatry* **62**, 168-  
518 178 (2007).
- 519 47 Di Maio, R. *et al.* alpha-Synuclein binds to TOM20 and inhibits mitochondrial protein import in  
520 Parkinson's disease. *Science translational medicine* **8**, 342ra378,  
521 doi:10.1126/scitranslmed.aaf3634 (2016).
- 522 48 Grassi, D. *et al.* Identification of a highly neurotoxic alpha-synuclein species inducing  
523 mitochondrial damage and mitophagy in Parkinson's disease. *Proceedings of the National*  
524 *Academy of Sciences of the United States of America* **115**, E2634-E2643,  
525 doi:10.1073/pnas.1713849115 (2018).
- 526 49 Tapias, V. *et al.* Synthetic alpha-synuclein fibrils cause mitochondrial impairment and selective  
527 dopamine neurodegeneration in part via iNOS-mediated nitric oxide production. *Cellular and*  
528 *molecular life sciences : CMLS* **74**, 2851-2874, doi:10.1007/s00018-017-2541-x (2017).
- 529 50 Ludtmann, M. H. R. *et al.* alpha-synuclein oligomers interact with ATP synthase and open the  
530 permeability transition pore in Parkinson's disease. *Nature communications* **9**, 2293,  
531 doi:10.1038/s41467-018-04422-2 (2018).
- 532 51 Castrioto, A., Thobois, S., Carnicella, S., Maillet, A. & Krack, P. Emotional manifestations of PD:  
533 Neurobiological basis. *Movement disorders : official journal of the Movement Disorder Society*  
534 **31**, 1103-1113, doi:10.1002/mds.26587 (2016).
- 535 52 Campos, F. L. *et al.* Rodent models of Parkinson's disease: beyond the motor symptomatology.  
536 *Frontiers in behavioral neuroscience* **7**, 175, doi:10.3389/fnbeh.2013.00175 (2013).
- 537 53 Caudal, D., Alvarsson, A., Bjorklund, A. & Svenningsson, P. Depressive-like phenotype induced by  
538 AAV-mediated overexpression of human alpha-synuclein in midbrain dopaminergic neurons.  
539 *Experimental neurology* **273**, 243-252, doi:10.1016/j.expneurol.2015.09.002 (2015).

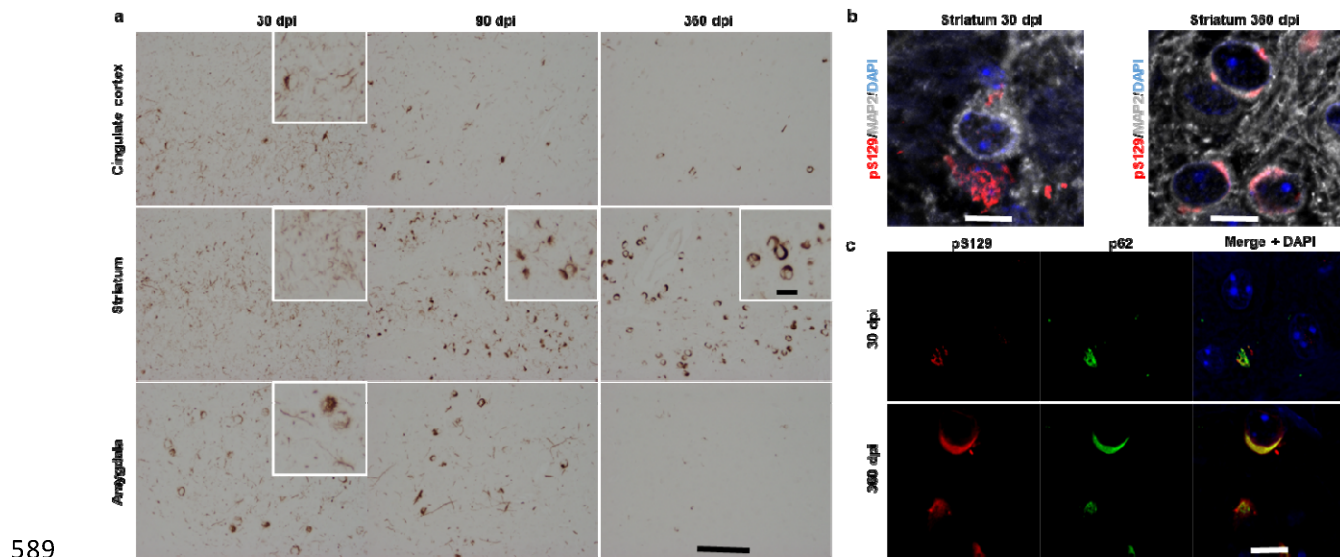
- 540 54 Janakiraman, U. *et al.* Influences of Chronic Mild Stress Exposure on Motor, Non-Motor  
541 Impairments and Neurochemical Variables in Specific Brain Areas of MPTP/Probenecid Induced  
542 Neurotoxicity in Mice. *PLoS one* **11**, e0146671, doi:10.1371/journal.pone.0146671 (2016).
- 543 55 Mattila, P. M., Rinne, J. O., Helenius, H., Dickson, D. W. & Roytta, M. Alpha-synuclein-  
544 immunoreactive cortical Lewy bodies are associated with cognitive impairment in Parkinson's  
545 disease. *Acta neuropathologica* **100**, 285-290 (2000).
- 546 56 Jellinger, K. A. Alpha-synuclein pathology in Parkinson's and Alzheimer's disease brain: incidence  
547 and topographic distribution--a pilot study. *Acta neuropathologica* **106**, 191-201,  
548 doi:10.1007/s00401-003-0725-y (2003).
- 549 57 Gómez-Tortosa, E., Newell, K., Irizarry, M. C., Sanders, J. L. & Hyman, B. T.  $\alpha$ -Synuclein  
550 immunoreactivity in dementia with Lewy bodies: morphological staging and comparison with  
551 ubiquitin immunostaining. *Acta neuropathologica* **99**, 352-357 (2000).
- 552 58 Kovari, E. *et al.* Lewy body densities in the entorhinal and anterior cingulate cortex predict  
553 cognitive deficits in Parkinson's disease. *Acta neuropathologica* **106**, 83-88, doi:10.1007/s00401-  
554 003-0705-2 (2003).
- 555 59 George, S. *et al.* Alpha-synuclein transgenic mice exhibit reduced anxiety-like behaviour.  
556 *Experimental neurology* **210**, 788-792, doi:10.1016/j.expneurol.2007.12.017 (2008).
- 557 60 Graham, D. R. & Sidhu, A. Mice expressing the A53T mutant form of human alpha-synuclein  
558 exhibit hyperactivity and reduced anxiety-like behavior. *Journal of neuroscience research* **88**,  
559 1777-1783, doi:10.1002/jnr.22331 (2010).
- 560 61 Ardouin, C. *et al.* [Assessment of hyper- and hypodopaminergic behaviors in Parkinson's  
561 disease]. *Revue neurologique* **165**, 845-856, doi:10.1016/j.neurol.2009.06.003 (2009).

- 562 62 Nemani, V. M. *et al.* Increased expression of alpha-synuclein reduces neurotransmitter release  
563 by inhibiting synaptic vesicle reclustering after endocytosis. *Neuron* **65**, 66-79,  
564 doi:10.1016/j.neuron.2009.12.023 (2010).
- 565 63 Froula, J. M. *et al.* alpha-Synuclein fibril-induced paradoxical structural and functional defects in  
566 hippocampal neurons. *Acta neuropathologica communications* **6**, 35, doi:10.1186/s40478-018-  
567 0537-x (2018).
- 568 64 Greene, J. G., Porter, R. H., Eller, R. V. & Greenamyre, J. T. Inhibition of succinate dehydrogenase  
569 by malonic acid produces an "excitotoxic" lesion in rat striatum. *Journal of neurochemistry* **61**,  
570 1151-1154 (1993).
- 571 65 Riepe, M. W. *et al.* Increased hypoxic tolerance by chemical inhibition of oxidative  
572 phosphorylation: "chemical preconditioning". *Journal of cerebral blood flow and metabolism :*  
573 *official journal of the International Society of Cerebral Blood Flow and Metabolism* **17**, 257-264,  
574 doi:10.1097/00004647-199703000-00002 (1997).
- 575 66 Lago, T., Davis, A., Grillon, C. & Ernst, M. Striatum on the anxiety map: Small detours into  
576 adolescence. *Brain research* **1654**, 177-184, doi:10.1016/j.brainres.2016.06.006 (2017).
- 577 67 Nouraei, N. *et al.* Critical appraisal of pathology transmission in the alpha-synuclein fibril model  
578 of Lewy body disorders. *Experimental neurology* **299**, 172-196,  
579 doi:10.1016/j.expneurol.2017.10.017 (2018).
- 580 68 Fares, M. B. *et al.* Induction of de novo alpha-synuclein fibrillization in a neuronal model for  
581 Parkinson's disease. *Proceedings of the National Academy of Sciences of the United States of*  
582 *America* **113**, E912-921, doi:10.1073/pnas.1512876113 (2016).
- 583 69 Yun, S. *et al.* Stimulation of entorhinal cortex–dentate gyrus circuitry is antidepressive. *Nature*  
584 *medicine* **24**, 658 (2018).

585 70 Steiner, J. A., Quansah, E. & Brundin, P. The concept of alpha-synuclein as a prion-like protein:  
586 ten years after. *Cell and tissue research*, doi:10.1007/s00441-018-2814-1 (2018).

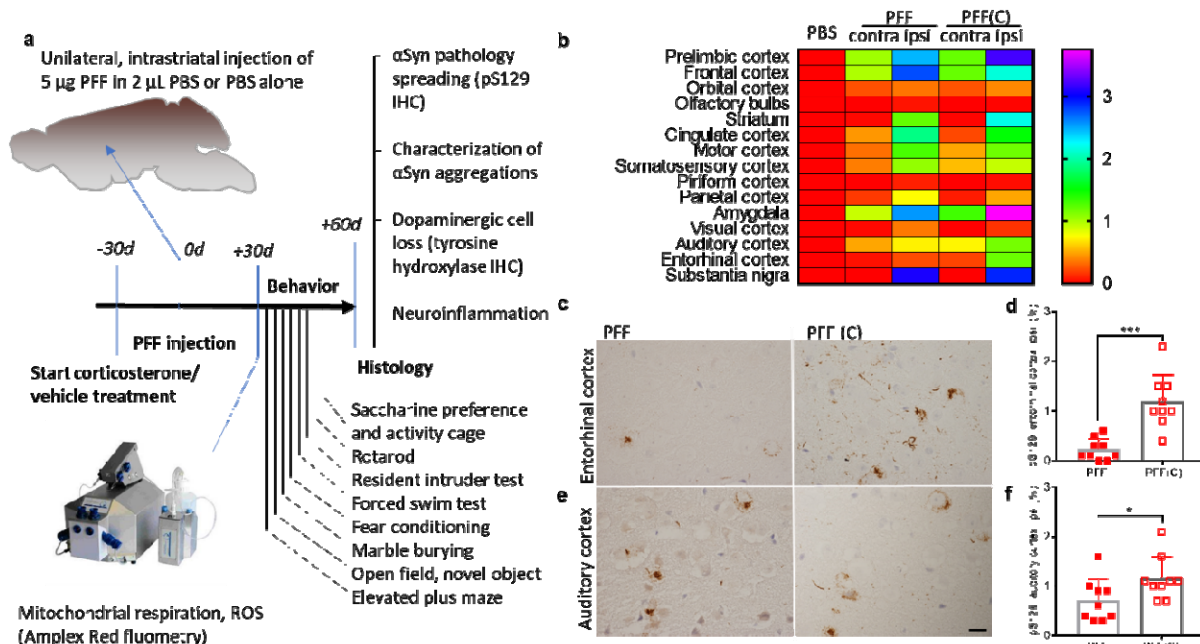
587

## 588 Figures



590 Fig. 1: Evolution of pS129 a-Syn pathology in the cingulate cortex, striatum and  
591 amygdala over time. (a)  $\alpha$ -Syn pS129 immunoreactivity in the cingulate cortex, striatum and  
592 amygdala (each in the hemisphere of injection) 30, 90 and 360 days post injection (dpi) after  
593 unilateral, intrastriatal injection of PFFs. (b) Striatal MAP2-positive (grey) neurons stained for  $\alpha$ -  
594 Syn pS129 (red) and at 30 and 360 dpi and (c) co-stained for  $\alpha$ -syn pS129 and p62. Scale bars  
595 are 100  $\mu$ m (a), 20  $\mu$ m (inset) and 10  $\mu$ m (b and c).

596



597

598 Fig. 2: Experimental setup and  $\alpha$ -Syn spreading pathology. (a) Experimental setup: 5  $\mu$ g of

599 PFFs in 2  $\mu$ L PBS (or PBS alone) were injected unilaterally in the dorsal striatum of mice that

600 were continuously treated with either corticosterone (35 mg/L) or vehicle (0.45%

601 hydroxypropyl- $\beta$ -cyclodextrin) in the drinking water throughout the experiment, starting 1

602 month before PFF/PBS-injection. 1 month after injections, some animals were sacrificed for

603 high-resolution respirometry experiments and the other group of animals was subjected to a

604 series of behavioral tests lasting for about another month, after which brains were processed

605 for histology (IHC = immunohistochemistry). (b) Heat map reflecting mean  $\alpha$ -Syn pathology

606 spreading across the brain, ipsi(lateral) and contra(lateral) (density of  $\alpha$ -Syn pS129

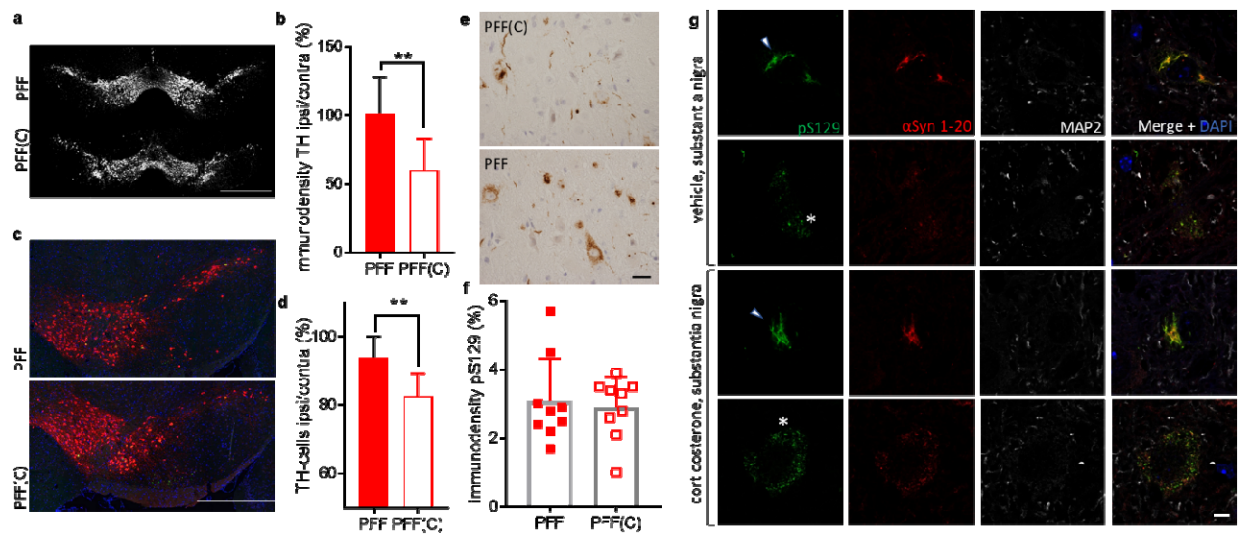
607 immunoreactivity in % of area). Significant differences in  $\alpha$ -Syn pathology spreading were

608 observed in 2 brain regions; entorhinal cortex (c,d; Mann-Whitney test,  $P < 0.001$ ) and auditory

609 cortex (e,f; Mann-Whitney test,  $P < 0.018$ ) between corticosterone- [PFF(C)] vs. vehicle- [PFF]

610 pretreated animals. Scale bar represents 20  $\mu$ m. N=9 mice per group.

611

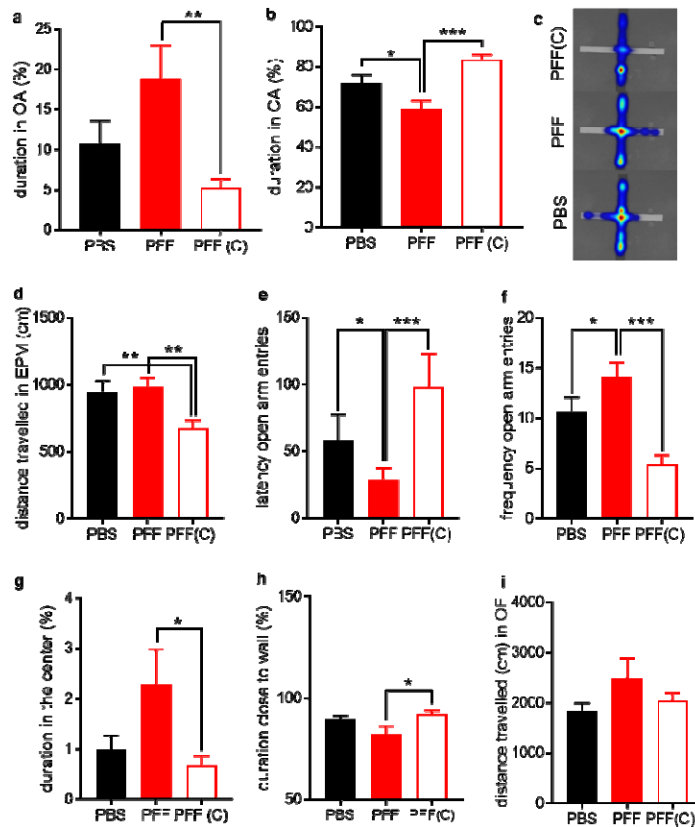


612

613 Fig. 3.  $\alpha$ -Syn preformed fibril (PFF) injections aggravated neuropathology in the  
 614 substantia nigra after chronic corticosterone (C). (a) Depictions of tyrosine hydroxylase  
 615 (TH)-labelled representative midbrains, including the substantia nigra and (b) quantification of  
 616 densities of TH immunoreactivity ( $p=0.003$ , t-test). (c) Micrographs of ipsilateral (i.e.  
 617 hemisphere of injection) midbrains including the substantia nigra, pars compacta and pars  
 618 reticulata (TH in red, pS129 in green and DAPI in blue) and (d) cell counts of ipsilateral  
 619 substantia nigra tyrosine hydroxylase positive neurons normalized to contralateral cell count  
 620 ( $p=0.002$ , t-test). Values reflect mean cell counts of 6 sections per brain each. (e)  $\alpha$ -Syn  
 621 pathology spreading (pS129 density) in the substantia nigra and quantification (f). (g)  
 622 characterization of aggregates in the substantia nigra using immunostaining for pS129,  $\alpha$ -Syn 1-  
 623 20 and microtubule associated protein 2 (MAP2) after proteinase K treatment. Note the two  
 624 clearly distinguishable aggregation forms: fibrillar (arrowheads) and granular (asterisks). Scale  
 625 bars represents 500  $\mu$ m (a,c), 20  $\mu$ m (e) and 5  $\mu$ m (g). N=9 per group for all quantifications.

626

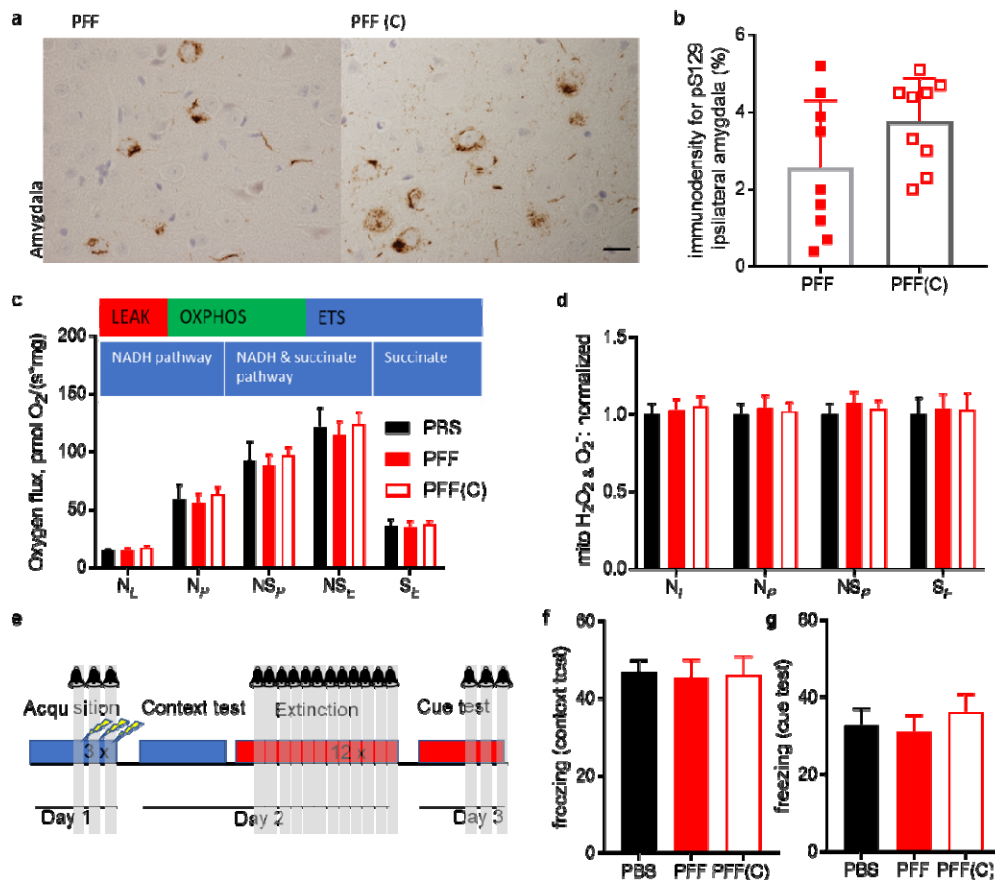
627



628

629 Fig. 4. Corticosterone (C) treatment reversed preformed fibril (PFF) induced anxiety-like  
 630 behaviors. A hypo-anxious phenotype in the elevated plus maze (EPM) of PFF-injected mice  
 631 was reversed by C-treatment, in the open arms (OA, a) and the closed arms (CA, b): 1way  
 632 ANOVAs,  $F(2, 51) = 5.384, P=0.008$  and  $F(2, 51) = 12.17, P<0.001$ . Representative heatmaps  
 633 visualizing visited areas in the EPM (warmer colors indicate higher presence of the mouse) (c).  
 634 C-treated and PFF injected mice moved less in the 7 min long EPM-test (d): 1way ANOVA,  $F(2,$   
 635  $51) = 3.46, P=0.005$ . Mice injected with PFF and pretreated with vehicle moved to the open  
 636 arms sooner than mice from the other groups (e); 1way ANOVA,  $F(2, 49) = 3.32, P=0.045$ . They  
 637 also visited the open arms more often (f); 1way ANOVA  $F(2, 51) = 11.81, P<0.001$ . (g) In the

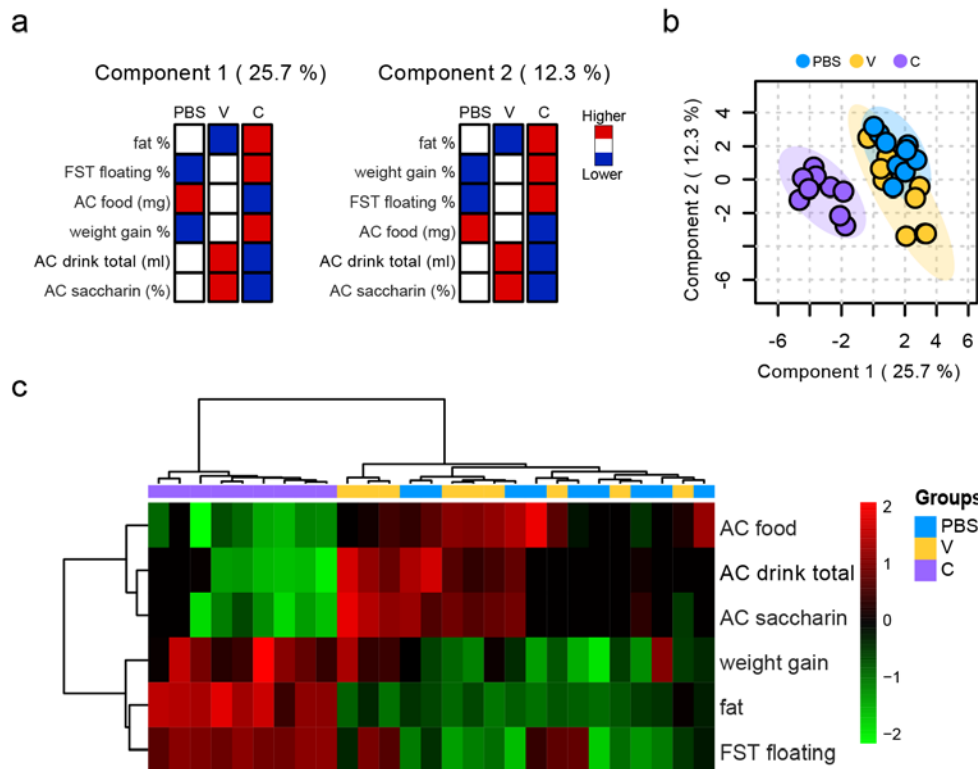
638 open field test (OF), mice injected with PFFs spent more time in the center, if not treated with C  
 639 (F (2, 24) = 3.604, P=0.043). Mice treated with C and PFFs accordingly spent more time close to  
 640 the walls (h), indicating higher anxiety-like behavior with C treatment: 1way ANOVA, F (2, 24) =  
 641 3.464, P=0.048. No differences between groups were observed for distance travelled in the OF.  
 642 N=17-18 per group for a-f, N=9 per group for g-i.



643  
 644 Fig. 5.  $\alpha$ -Syn pathology in the amygdala after PFF-injection does not affect  
 645 mitochondrial function and amygdala-related behaviors. (a) Similar  $\alpha$ -Syn pS129  
 646 immunoreactivities in the basolateral amygdala (scale bar represents 20  $\mu$ m) are quantified in  
 647 (b); P=0.14, Mann-Whitney. Mitochondrial respiration was assessed in LEAK and OXPHOS states  
 648 driven by the NADH pathway ( $N_L$  and  $N_p$ ), in the OXPHOS state driven by NADH and succinate



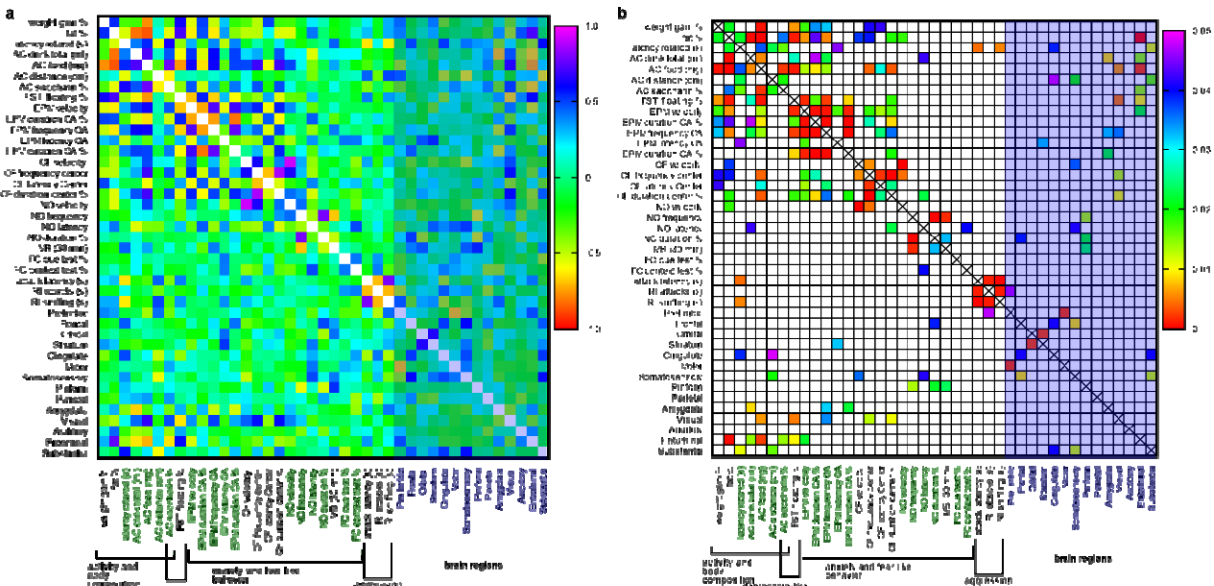
649 pathway combined ( $NS_p$ ), the electron transport system (ETS) state driven by NADH and  
 650 succinate pathway combined ( $NS_E$ ) or only by the succinate pathway ( $S_E$ ). No differences in  
 651 respiration were observed in any state across the groups (c). Amplex red fluorometry  
 652 performed in parallel to respiration revealed no differences in mitochondrial hydrogen peroxide  
 653 or superoxide production in any state (d): ROS-levels are normalized to PBS-injected controls  
 654 (no corticosterone (C) treatment). Neither  $\alpha$ -Syn pathology, nor additional CORT treatment  
 655 affected fear related behaviors (e-g). Scheme of fear conditioning experiments (e), freezing  
 656 behaviors in the context (f) and in the cue (g) test. N=8-9 per group.  
 657



658

659 Fig. 6: PLS Discriminant analysis results. Model accuracy was used to decide for the  
 660 number of components. Two components were chosen, resulting in a model accuracy of  
 661 approximately 76 %. Empirical p-value for using 2 components, estimated with permutation

662 statistics (N permutation = 2000,  $p=0.004$ ). (a) the 6 variables with highest variable importance  
 663 in projection (VIP) for each component used in the model and their respective contribution for  
 664 each experimental group: “fat” is the percentage of fat per body mass, “FST floating” is the  
 665 percentage of time in the FST (forced swim test) spent in immobility, “AC drink total” are  
 666 consumption (water and saccharine solution combined, in ml) in the AC (activity cage), “AC  
 667 saccharin” describes the percentage of saccharin solution consumed per total consumption of  
 668 water and saccharine solution combined, “AC food” is the total food consumed during the AC.  
 669 (b) Scatterplot depicting values of individual mice for the 2 components. (c) heat map of the  
 670 previous variables for each subject (each column summarized data of 1 animal). Corticosterone  
 671 (C) and vehicle (V) pretreated mice injected with PFFs and the PBS-injected control group are  
 672 compared.  
 673



674  
 675 Fig. 7. Correlations between behavioral measures and  $\alpha$ -Syn pS129 immunoreactivity in  
 676 specific brain regions of animals injected with  $\alpha$ -Syn preformed fibrils (corticosterone

677 and vehicle pretreated cohorts pooled). Pearson's correlation coefficients are represented in

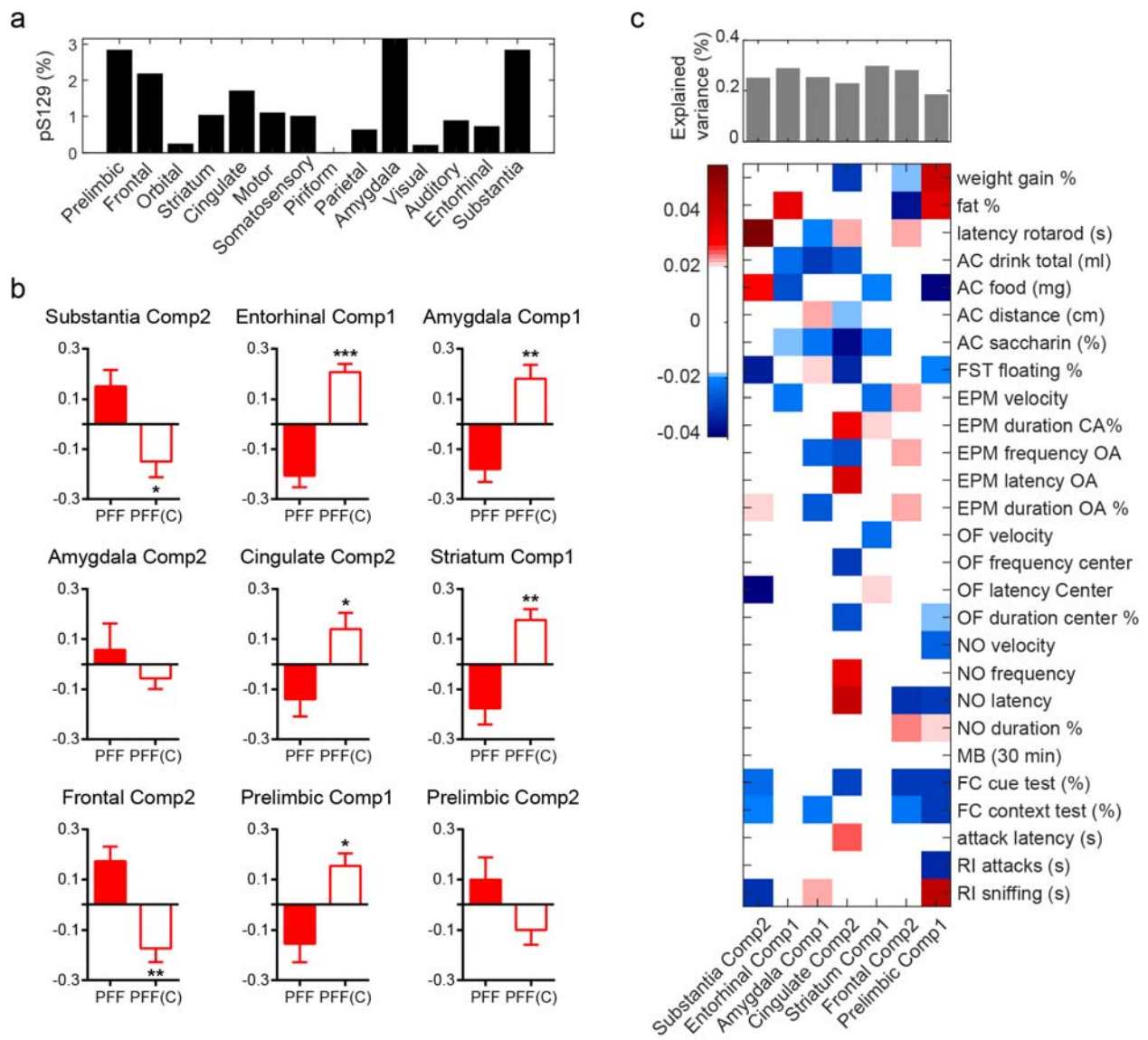
678 (a), while according P-values (<0.05) are indicated in (b). AC = activity cage, FST = forced swim

679 test, EPM = elevated plus maze, OF = open field test, NO = novel object test, MB = marble

680 burying test, FC = fear conditioning, Ctx = cortex

681

682



683

684 Fig. 8: PLS Regression components with significant group differences on PFF-injected  
685 animals. a) Mean values of  $\alpha$ -Syn pS129 immunoreactivity (% of area) for selected brain  
686 regions; b) Group differences [PFF vs. PFF(C) groups] for PLS component (Comp) values with  
687 percentage of variance explained larger than 15%. ANOVA tests following a significant MANOVA  
688 ( $P=0.003$ ) with P-values corrected for multiple comparisons with the Holm–Bonferroni method;  
689 c) percentage of variance explained (top bar plot) and weights (bottom matrix) of the PLS  
690 regression components for each brain region where there was a significant effect of Group.  
691 AC = activity cage, FST = forced swim test, EPM = elevated plus maze, OF = open field test, NO =  
692 novel object test, MB = marble burying test, FC = fear conditioning, RI = resident intruder test  
693 Significance levels: \*  $p < 0.05$ ; \*\*  $p < 0.01$ ; \*\*\*  $p < 0.001$

694

## 695 Materials and methods

696

### 697 Preparation and Characterization of PFFs

698  $\alpha$ -Syn PFFs were generated from recombinant mouse (m)  $\alpha$ -Syn protein. The lyophilized protein  
699 was dissolved in PBS at a concentration of 325  $\mu$ M and set to pH7.2. The solution was  
700 centrifuged for 5 min through a 0.2  $\mu$ M filter at 5000 rpm and purity was confirmed by mass  
701 spectrometry and HPLC. Supernatant was incubated under constant agitation of 900 rpm on an  
702 orbital shaker at 37°C for 4 days. The generated m $\alpha$ -Syn fibrils were sonicated briefly (40%  
703 amplitude, one pulse for 5 s) and then were aliquoted and stored at -80 °C.

704 Thioflavin T (ThT) binding was performed to assess amyloid formation with excitation at 450  
705 nm, emission at 485 nm (Bucher Analyst AD plate reader). Samples were treated with ThT (10  
706  $\mu$ M, in 50 mM glycine, pH8.5) in black 384-well plates (Nunc).  
707 Remaining soluble protein was assessed by sedimentation assay (supernatant after  
708 centrifugation at 100000g for 30 min) and filtration assay (14000 g for 15 min through a 100 kD  
709 filter) and analysed by SDS-PAGE (15% polyacrylamide gel) and Coomassie (Life Technologies)  
710 staining.  
711 Samples were applied on glow-discharged Formvar/carbon-coated 200-mesh copper grids for  
712 analysis by transmission electron microscopy.

713

#### 714 **Animals and surgical procedure**

715 C57BL/6JRj male mice were ordered at an age of 8 weeks (Elevage Janvier) and allowed to  
716 acclimate to the animal house for at least 2 weeks. They were kept at 23 °C (40 % humidity) in a  
717 12h/12h light/dark cycle (7am-7pm and 7pm -7am, respectively) and free access to standard  
718 laboratory rodent chow and water, 3 animals per cage. For the resident intruder test younger  
719 BalbC mice (10 -12 weeks at test; 3 per cage) and female C57BL/6JRj (3 months old at test) were  
720 purchased 2 week before the test.

721 All animal experimentation procedures were approved by the Cantonal Veterinary Authorities  
722 (Vaud, Switzerland) and performed in compliance with the European Communities Council  
723 Directive of 24 November 1986 (86/609EEC). Every effort was taken to minimize the number of  
724 animals used.

725 Surgical procedures were performed at an age of 3-5. Wild-type  $\alpha$ -Syn PFFs were stereotaxically  
726 injected unilaterally into the right dorsal striatum (coordinates: AP +0.4, ML +2, DV -2,6). Fully  
727 anesthetized animals (100 mg/kg ketamine and 10 mg/kg xylazine, i.p.) were mounted on  
728 stereotactic frames (Kopf Instruments), lubricant eye ointment (Viscotears) was applied and 5  
729  $\mu$ g PFFs in 2  $\mu$ L PBS were injected using a 10  $\mu$ L Hamilton syringe attached to a 34-gauge canula  
730 at a flow rate of 0.1  $\mu$ L/min. Skin incisions were sutured with dissolvable stitches (Vicryl 6.0). All  
731 animals were monitored until fully awake and treated with paracetamol (200-300 mg/kg; 2  
732 mg/ml) in the water bottle for 3 days after surgery.

733 After behavioural experiments (N=9 per group), animals were killed by an overdose of  
734 thiopental (150 mg/kg) and after removing blood with heparinized saline (0.9%) brains were  
735 fixed by transcardial perfusion with 4 % paraformaldehyd for immunohistochemistry and  
736 histological studies. Mice for mitochondrial respiration studies (N=8-9 per group) were killed by  
737 neck dislocation and used immediately to measure oxidative phosphorylation parameters.

### 738 [Assessment of body composition](#)

739 Body weight of animals was continuously assessed throughout the experiments. Fat- and lean-  
740 mass was measured by Echo MRI at start of corticosterone/vehicle treatment (considered for  
741 randomization to experimental groups) and 3 weeks after surgery.

### 742 [Continuous exogenous corticosterone treatment](#)

743 Corticosterone (CORT, Sigma) was dissolved in 0.45 % hydroxypropyl- $\beta$ -cyclodextrin (Sigma).  
744 Either corticosterone (35 mg/l) in hydroxypropyl- $\beta$ -cyclodextrin or hydroxypropyl- $\beta$ -  
745 cyclodextrin alone (vehicle) was administered to animals in drinking water starting 4 weeks

746 before surgery and then continuously until sacrifice of the animals as described elsewhere  
747 (Bacq et al, 2012).

## 748 Behavioral tests

749 Starting 4 weeks before surgery, animals were handled weekly (removed from the cage gently,  
750 occasionally weighed) until start of behavioural testing and weighed weekly until the end of  
751 behavioural tests. All behavioural tests were performed in the morning (8am-1pm), unless  
752 stated otherwise. Camcorders (Sony) were used to record behaviour, where applicable.

## 753 Elevated plus maze

754 Mice were habituated to the experimental room for at least 45min. They were then placed in  
755 the central area of an elevated plus maze (65 cm above the floor, with 2 open and 2 enclosed  
756 arms) and allowed to explore the maze for 5 minutes. Maze was cleaned with 5% ethanol  
757 between runs. Exploratory behaviour and the time spent in each arm or the center was  
758 recorded. Lux in distal parts of open arms was 12.1-12.2 and 8.7 at the mid junction. Ethovision-  
759 software (Noldus) was used to score behavior.

## 760 Open field and novel object test

761 Light intensity was adjusted to 7 lux in the center of squared boxes. Mice were habituated to  
762 the experimental room for more than 30 min before the test and were then placed in the open-  
763 field arena. After 10 min a novel object (transparent drinking bottle) was placed in the middle  
764 of the arena and mice were again allowed to explore freely for 5 min. Distance travelled and  
765 the time spent in the different areas defined in the arena (wall, intermediate and center) were  
766 recorded. Ethovision-software (Noldus) was used to score behavior.

## 767 **Marble burying test**

768 Experimental cages were filled approximately 4-5 cm high with bedding. Mice were habituated  
769 to the testing room at least 30 minutes before the test. For 15 min, mice were allowed to  
770 explore the experimental cage (in absence of marbles). Mice were removed from the cages, 12  
771 glass marbles were placed per cage in a regular pattern on the surface of bedding material,  
772 evenly spaced around 4 cm apart, after which the mouse was put back into the cage for 45  
773 minutes. The number of visible marbles was assessed throughout the time of the experiment.

## 774 **Fear conditioning**

775 Mice were habituated to the conditioning chamber for at least for 30 min before each  
776 experiment.

777 (1) Fear acquisition was performed in transparent conditioning chambers equipped with metal  
778 grids on a floor plate and cleaned before each trial with 5% ethanol. 3 min after a mouse was  
779 placed into the chamber, it was exposed to a 30 s (800 Hz, 80 dB) long auditory cue (Acoustic  
780 Stimuli LE 114, Panlab, s.l.), followed by a 2 s, 0.5 mA electrical foot shock (Shocker LE 100-26,  
781 Letica) delivered via the metal grid. 1 and 2.5 min later auditory cue and foot shock were  
782 repeated.

783 (2) Context test was performed 1 day later in the same context as in fear acquisition. Mice were  
784 placed for 7.5 min in the conditioning chamber without auditory cues or foot shocks being  
785 delivered. Chambers were cleaned before each trial with 5% ethanol.

786 (3) Extinction training was performed on the same day in the afternoon in a new context: room  
787 light was dimmed, the floor grid was replaced by a white floor plate, 5% vanilla-solution was



788 used for cleaning. A circular cage with jungle-like painting was used instead of the transparent  
789 chambers. 3 min after a mouse was placed in the conditioning chamber, it was exposed to 12  
790 consecutive 30 s long auditory cues (same as in fear acquisition), interspersed by silent phases  
791 of 1 min each.

792 (4) In the next morning, mice were placed in the same context as for extinction training, 5%  
793 vanilla-solution was used for cleaning. 3 min after a mouse was placed into the chamber, it was  
794 exposed to 3 consecutive 30 s long auditory cues (same as in fear acquisition), interspersed by  
795 silent phases of 1 min each.

796 Softwares *Freezing v1.3.05* and *The Observer XT 11.5* were used to program the different  
797 protocols and to analyze fear behavior, respectively. Freezing was defined as the absence of all  
798 movement, except for breathing. All sequences with tone exposure were scored for acquisition,  
799 extinction and tone test. Context test was scored entirely.

#### 800 **Forced swim test**

801 5 L glass beakers were filled with 3-3.5 L tap water (25°C). Mice were exposed to the water for  
802 15 min on day 1 and another 5 min on the following day. *Ethovision* (Noldus) software was used  
803 to quantify immobile floating versus active swimming behavior.

#### 804 **Resident intruder test**

805 Tested male mice (residents) were housed in a standard cage with a female for 4 days prior to  
806 the test to facilitate the development of territoriality. The bedding of the cage was not changed  
807 during that initial period. On the day of the test, the female was removed from the cage. 30 min

808 later, an unfamiliar younger, male BalbC (intruder) with 5-15% less weight was introduced into  
809 the home cage. The two mice were allowed to interact physically for 10 min.

810 Resident intruder tests were performed exclusively within the dark period of the animal house  
811 (between 7pm and 1am).

## 812 Rotarod

813 Animals were habituated to the experimental room for at least 30 min. Mice were placed on  
814 the lanes of a Rotarod apparatus (BIOSEB) rod with an empty lane between each mouse. During  
815 training and testing, the same mouse was always put on the same lane. Acceleration speed was  
816 set to 4-40 rpm. 3 trials were realized for each mouse, with an inter-trial break of 15 min.

817 Maximum trial duration was 300 s. The apparatus was cleaned between each trial with 5%  
818 mucosol.

819 On day 1 animals were trained to stay on the rotarod rod. Training was stopped in case of three  
820 consecutive times of the following events: passive rotation, jumping off, or falling off the rod.

821 Animals were tested 1 day later, 3 trials each. Each test was ended, when the mouse passively  
822 rotated, jumped or fell off the rod or if 300 s elapsed. For analysis, only day 2 was used. The  
823 average of the best 2 trials were used for analysis.

## 824 Activity cage and saccharin preference

825 Mice were single caged in an activity cage (TSE-systems) for 72 h. By means of a two-bottle  
826 preference test intake of saccharin solution (0.05% saccharin sodium salt, Sigma) was compared  
827 with intake of tap water. Additionally, overall drinking and food consumption of the mice was

828 recorded and general motor activity was assessed. All parameters were recorded in 30 min  
829 intervals.

## 830 **Respirometry**

831 Mice for respirometric experiments were sacrificed by neck dislocation and amygdala and  
832 striatum were dissected on ice using a mouse brain matrix (Agnthos). Wet tissue was weighed  
833 and collected in ice-cold BIOPS (2.8 mM Ca<sub>2</sub>K<sub>2</sub>EGTA, 7.2 mM K<sub>2</sub>EGTA, 5.8 mM ATP, 6.6 mM  
834 MgCl<sub>2</sub>, 20 mM taurine, 15 mM sodium phosphocreatine, 20 mM imidazole, 0.5 mM  
835 dithiothreitol and 50 mM MES, pH = 7.1), homogenized in ice-cold MiR05 (0.5 mM EGTA, 3mM  
836 MgCl<sub>2</sub>, 60 mM potassium lactobionate, 20 mM taurine, 10 mM KH<sub>2</sub>PO<sub>4</sub>, 20 mM HEPES, 110 mM  
837 sucrose and 0.1% (w/v) BSA, pH=7.1) using a pestle for eppendorf tubes in a concentration of 1  
838 mg wet-weight per 10 µL MiR05. Respiration was measured in parallel to mitochondrial ROS  
839 production (O<sub>2</sub><sup>-</sup> and H<sub>2</sub>O<sub>2</sub>) at 37 °C in the Oroboros O2k equipped with the O2K Fluo-LED2  
840 Module (Oroboros Instruments, Austria). For mitochondrial ROS-measurement LEDs for green  
841 excitation were applied and a concentration of 1 mg wet tissue per ml MiR05 was added to final  
842 concentrations of 10 µM amplex red, 1 U/ml horse radish peroxidase and 5 U/ml superoxide  
843 dismutase in 2 ml MiR05 per O2K chamber. Calibration was performed by titrations of 5 µL of  
844 40 µM H<sub>2</sub>O<sub>2</sub>.

845 A substrate-uncoupler-inhibitor-titration (SUIT) protocol was applied to measure oxygen flux at  
846 different repirational states as described previously (Hollis et al, 2015; Burtscher et al, 2015).  
847 Briefly, NADH-pathway (N) respiration in the LEAK and oxidative phosphorylation (OXPHOS)  
848 state was analysed in presence of malate (2mM), pyruvate (10mM) and glutamate (20mM)  
849 before and after the addition of ADP (5 mM), respectively (N<sub>L</sub>, N<sub>p</sub>). Addition of succinate (10

850 mM) allowed assessment of NADH- and Succinate-linked respiration in OXPHOS ( $NS_p$ ) and in the  
851 uncoupled state ( $NS_E$ ) after incremental ( $\Delta 0.5 \mu\text{M}$ ) addition of carbonyl cyanide m-chlorophenyl  
852 hydrazine (CCCP). Inhibition of Complex I by rotenone ( $0.5 \mu\text{M}$ ) yielded succinate-linked  
853 respiration in the uncoupled state ( $S_E$ ). Tissue-mass specific oxygen fluxes were corrected for  
854 residual oxygen consumption,  $R_{ox}$ , measured after additional inhibition of the mitochondrial  
855 electron transfer system, ETS, Complex III with antimycin A. For further normalization, fluxes of  
856 all respiratory states were divided by ET-capacity to obtain flux control ratios,  $FCR$ .

857 Terminology was applied according to

858 [http://www.mitoeagle.org/index.php/MitoEAGLE\\_preprint\\_2018-02-08](http://www.mitoeagle.org/index.php/MitoEAGLE_preprint_2018-02-08).

859

## 860 Brain tissue preparation for gel electrophoresis and western blots

861 Brain homogenates not used for respirometry were treated with protease and phosphatase  
862 inhibitors, snap-frozen and stored at  $-80^\circ\text{C}$ . Protein concentrations were determined by BCA  
863 assay (Thermo Scientific), samples were diluted in 4x Laemmli buffer, boiled for 10 min and  
864 separated on a 15% SDS-PAGE gel and transferred onto nitrocellulose membrane (Fisher  
865 Scientific, Lucens, Switzerland) with a semi-dry system (Bio-Rad, Crissier, Switzerland).  
866 Membranes were probed overnight at  $4^\circ\text{C}$  with the primary antibody of interest after 30 min  
867 of blocking in Odyssey blocking buffer (Li-Cor Biosciences, Bad Homburg, Germany) diluted  
868 1:23 in PBS. After four washes with PBS and 0.01% (v/v) Tween-20 (PBS-T), membranes were  
869 incubated for 1 h with secondary antibodies (goat Alexa Fluor<sup>680</sup> IgG) protected from light at

870 RT. Immunoblots were finally washed 4 times with PBS-T and scanned using a Li-COR scanner  
871 (Li-Cor Biosciences) at a wavelength of 700nm. Image J was used for densitometry.

## 872 Immunohistochemistry and imaging

873 Immunohistochemistry and Mayer's hematoxylin stainings were performed on sections of  
874 brains fixed in 4% paraformaldehyde, embedded in paraffin and cut coronally to 4 µm. Sections  
875 were de-waxed and epitope retrieval was performed for 20 min at 95°C in trisodium citrate  
876 buffer (10mM, pH 6.0) in a retriever (Labvision). Sections were then blocked for 60 min in 3%  
877 bovine serum albumin in PBS containing 0.1% Triton X-100 at RT. Primary antibodies were  
878 applied over night at 4°C and secondary antibodies for immunofluorescence for 60 min at RT,  
879 before mounting the slides using fluoromount. In case of 3,3'-diaminobenzidine (DAB) –  
880 revelation, sections were exposed to 3% H<sub>2</sub>O<sub>2</sub> in PBS for 30 min before blocking and ImmPRESS  
881 reagent anti-mouse IgG (Vector MP-7402) or anti-goat IgG (Vector MP-7405) was applied for 40  
882 min at RT instead of fluorescent secondary antibodies, followed by incubation for 10 min in DAB  
883 dissolved in 50 mM Tris buffer and 0.06% H<sub>2</sub>O<sub>2</sub>. Sections were counterstained with Mayer's  
884 hematoxylin and mounted with fluoromount. In case of Proteinase K (PK) treatment, sections  
885 were incubated for 8 min at room temperature in 1 µg/mL of PK in 50mM TrisHCl buffer (pH  
886 7.4).

887 Tiled images for TH were produced with a Leica DM5500 microscope, an Olympus AX70  
888 microscope was used to create images from DAB-stained sections and Zeiss LSM700 confocal  
889 microscopes or Leica DM5500 were used to image immunofluorescent sections. Image J was  
890 used to assess densities of immunoreactivity (coverage of area with immunoreactivity in % of  
891 total area).

892

893 Table 1: antibodies employed

type	species	specification	Concentration	application
aSyn pS129	mouse	Wako 014-20281	1:10000  (DAB), 1:1000  (IF)	IHC
Tyrosine hydroxylase	rabbit	Millipore AB152	1:1000	IHC
MJF-R13	rabbit	Abcam 168381	1:750	IHC
MAP2	chicken	Abcam ab5392	1:2000	IHC
GFAP	goat	Santa Cruz sc-6170	1:500	IHC
Ubiquitin 1	mouse	Millipore MAB1510	1:500	IHC
p62	mouse	Abcam ab56416	1:1000	IHC
aSyn 1-20	rabbit	Eurogentec	1:1000	IHC
antiRabbit 647	donkey	Invitrogen	1:800	IHC
antiMouse 488	goat	Invitrogen	1:800	IHC
antiMouse 568	goat	Invitrogen	1:800	IHC
antiChicken 488	donkey	Jackson lab	1:500	IHC
ImmPRESS antiMouse	horse	Vector MP-7402	1 drop /  section	IHC
ImmPRESS antiGoat	horse	Vector MP-7405	1 drop /  section	IHC

Synuclein (SYN1)	mouse	BD Transduction, BD610787	1:1000	Western blot
Beta-actin	mouse	Abcam Ab6276-100	1:5000	Western blot
anti-mouse 680 IRDye 680RD	goat	Li-COR 926-68070	1:10000	Western blot

894

## 895 **Statistical analyses**

896 Data are presented as means  $\pm$  SD, except for behavioural tests, in which means  $\pm$  SEM are  
897 presented. Heat maps are based on mean values (of pS129 immunodensities for brain regions).

898 Statistical tests applied for the different experiments are given in figure legends. P values  $<0.05$   
899 were considered as significant. Pearson coefficients were calculated for correlation studies.

900 Microsoft Office Excel and Graphpad Prism were used to present statistical results, except for  
901 PLS-analyses (see below).

## 902 **PLS Discriminant analysis**

903 Partial least squares discriminant analysis (PLS-DA) was used to determine which of the  
904 behavioral and physiological variables assessed in this study best discriminate among PFF  
905 injected groups (CORT and vehicle) and PBS-injected controls (vehicle). For each variable, mean  
906 value imputation was used, missing scaling was performed by mean centering and dividing by  
907 the square root of the standard deviation (z-scoring).

908 The cross validation (CV) procedure performed was the 10-fold CV, with prediction accuracy as  
909 the measured performance metric. PLS-DA model validation relied on permutation tests using  
910 2000 permutations where, for each permutation, a PLS-DA model is built for the data with  
911 permuted group labels, and its prediction accuracy is calculated. The null-hypothesis of a non-  
912 significant discriminant model is rejected if the prediction accuracy with the original groups is  
913 not a part of the distribution based on the permuted group assignment (above the 95<sup>th</sup>  
914 percentile).

915 Analysis was performed in MetaboAnalyst 4.0 (<http://www.metaboanalyst.ca>)

#### 916 PLS Regression analysis

917 Partial least squares (PLS) regression was used to analyze levels of  $\alpha$ -Syn pS129  
918 immunoreactivity for PFF-injected groups in pre-selected brain regions behavior variables. For  
919 each variable, mean value imputation was used, missing scaling was performed by mean  
920 centering and dividing by the square root of the standard deviation (z-scoring). For each brain  
921 region, the resulting PLS components with a percentage of variance explained larger than 15%  
922 were selected and used as the dependent variable in a multivariate analysis of variance  
923 (MANOVA) using the PFF(C) group as the independent variable and all the pre-selected  
924 components as dependent variables. Follow-up ANOVAs based on a significant MANOVA  
925 outcome were corrected for multiple comparisons (Holm–Bonferroni method). PLS regression  
926 was implemented with the Matlab (version 2018a) function *plsregress*.